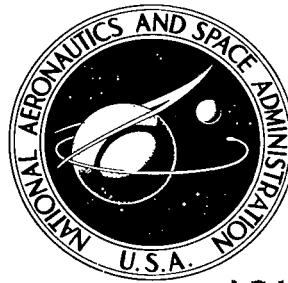


NASA TECHNICAL NOTE



NASA TN D-4469

c.1

LOAN COPY: RE  
AFWL (WL  
KIRTLAND AFB

0131057



TECH LIBRARY KAFB, NM

NASA TN D-4469

# THE OPERATION OF AN ELECTRON PARAMAGNETIC RESONANCE SPECTROMETER

*by F. E. Geiger, Jr.*

*Goddard Space Flight Center  
Greenbelt, Md.*





THE OPERATION OF AN ELECTRON  
PARAMAGNETIC RESONANCE SPECTROMETER

By F. E. Geiger, Jr.

Goddard Space Flight Center  
Greenbelt, Md.

NATIONAL AERONAUTICS AND SPACE ADMINISTRATION

---

For sale by the Clearinghouse for Federal Scientific and Technical Information  
Springfield, Virginia 22151 - CFSTI price \$3.00

## ABSTRACT

This paper discusses the operation of an electron paramagnetic resonance microwave spectrometer and gives expressions for the signal obtained from a paramagnetic sample with RF susceptibility  $\chi = \chi' - j\chi''$ . Calculations are made to the second order of  $\chi''$  and  $\chi'$ . Also studied are the effect of relative microwave power in the signal arm and in the bias or reference arm of the microwave bridge, and the effects of crystal detector characteristics on the optimum cavity reflection coefficient. Expressions for signals are developed for balanced-bridge operation with small phase or amplitude unbalance and for bridge operation with biasing arrangements for the detecting crystal.

## CONTENTS

Abstract .....	ii
INTRODUCTION .....	1
CALCULATION OF RESONANCE SIGNAL.....	1
SIGNAL DETECTION WITH LARGE CRYSTAL BIASING VOLTAGE .....	3
Case 1: Large Bias, Absorption.....	4
Case 2: Large Bias, Dispersion.....	4
SIGNAL DETECTION WITH BALANCED BRIDGE .....	6
Case 3: Balanced Bridge, Absorption .....	6
Case 4: Balanced Bridge, Dispersion .....	6
OPTIMUM CAVITY REFLECTION COEFFICIENT AT RESONANCE AND CRYSTAL CHARACTERISTICS .....	7
CONCLUSIONS .....	9
References .....	10
Appendix A—1N23WE Crystal Characteristics.....	11

# THE OPERATION OF AN ELECTRON PARAMAGNETIC RESONANCE SPECTROMETER

by

F. E. Geiger, Jr.

*Goddard Space Flight Center*

## INTRODUCTION

A number of papers have discussed electron paramagnetic resonance (EPR) microwave bridge spectrometers and the signals obtained from them for substances with RF susceptibility  $\chi = \chi' - j\chi''$ . This paper attempts, in a general manner, to derive the optimum conditions for observing the dispersion and absorption signal due to this complex susceptibility in a general way without recourse to the special relation between the power  $P$  absorbed by the spin system, and the absorptive part of the complex susceptibility,  $\chi''$ . That is,  $P = 2\omega H_1^2 \chi'' V_s$ , where  $\omega$  is the angular frequency,  $H_1$  is the amplitude of the magnetic radio frequency field, and  $V_s$  is the volume of the paramagnetic sample. The signal from the bridge is obtained to the second order of  $\chi'$  and  $\chi''$ , and the effect of detection crystal bias on these unwanted terms is discussed.

The results are compared with those obtained by Weger (Reference 1) for signals containing second-order terms of the dispersion and absorption. Spectrometer signal voltages are obtained for balanced bridge operation (square-law detection) and for operation with proper biasing voltages on the crystal detector ("linear" detection). The optimum value of the cavity reflection coefficient for maximum signal is examined as a function of crystal characteristics and of the relative amounts of power in the sample and reference or biasing arm of the microwave bridge. The analysis of the bridge circuit proceeds according to Goldsborough and Mandel (Reference 2).

## CALCULATION OF RESONANCE SIGNAL

In calculating the resonance signal, a simple microwave bridge configuration as shown in Figures 1 and 2 is assumed. Figure 1 represents the usual magic "T" bridge in which crystal bias and bridge balance are obtained with the slide-screw tuner in the reference arm or with an equivalent arrangement (Reference 3). Figure 2 illustrates a similar arrangement where the reference arm is replaced with a separate bias arm (References 3 and 4). Both circuits use a reflection cavity containing the paramagnetic sample. The cavity-coupling system, transmission line (waveguide), and signal generator may be represented by the usual lumped-constant equivalent circuit (References 2, 5, and 6) as shown in Figure 3, with components  $R$ ,  $L$ ,  $C$ , and characteristic line

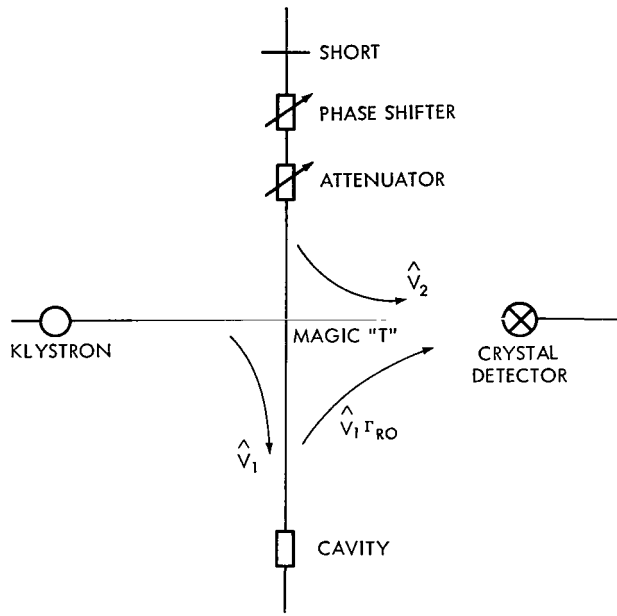


Figure 1—Magic "T" microwave bridge.

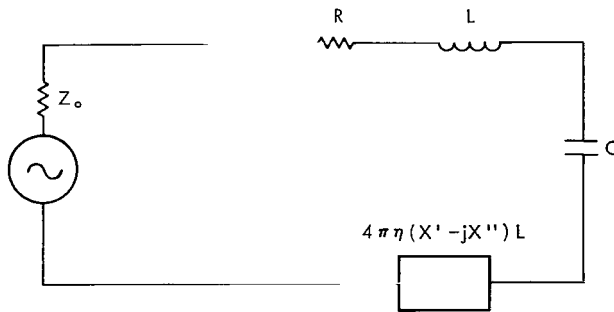


Figure 3—Microwave bridge equivalent circuit.

incident on the detecting crystal. When the paramagnetic sample passes through electron spin resonance, the lumped parameter  $L$  of the cavity changes by  $(4\pi\eta)L(X' - jX'')$  (Reference 7), where a term containing the static magnetic susceptibility  $\chi_0$  has been neglected. The equivalent circuit of the cavity and transmission line and the change in  $L$  due to the sample are shown in Figure 3. The total impedance of the cavity and coupling circuit will be

$$Z(\omega) = R + j\omega L(1 + 4\pi\eta X') + \omega L 4\pi\eta X'' - j(1/C\omega), \quad (2)$$

where  $\eta$  is a filling factor that depends on the oscillating magnetic field distribution in the cavity and the sample volume and  $jLX''$  and  $LX'$  are the absorptive and dispersive changes in  $L$ , respectively, due to resonance. If  $(1/LC)^{1/2}$  is replaced by  $\omega_0$ , the resonance frequency of the cavity,

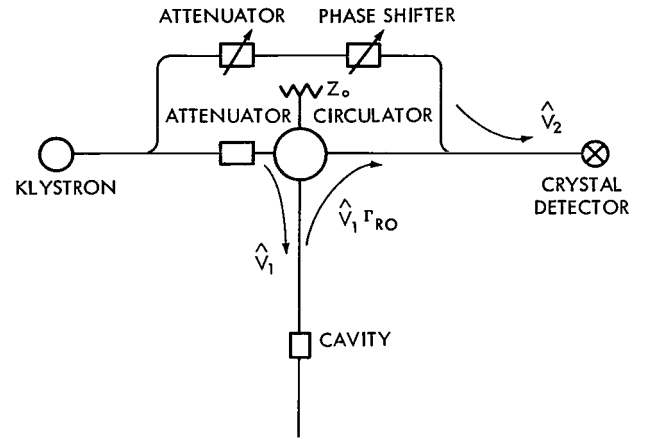


Figure 2—Microwave bridge with circulator and bias arm.

impedance  $Z_0$ . It is convenient to express the equivalent cavity parameters in terms of experimentally determinable  $Q$ -factors and to calculate the microwave signal derived from the paramagnetic sample in terms of these  $Q$ -factors. They are defined as follows (Reference 2):

$$\begin{aligned} Q_U(\text{unloaded}) &= (\omega L/R), \\ Q_E(\text{external}) &= (\omega L/Z_0), \\ Q_L(\text{loaded}) &= \omega L/(Z_0 + R). \end{aligned} \quad (1)$$

We shall first calculate the signal reflected from the cavity, and then find the total voltage

then

$$Z(\omega) = R + 4\pi\eta\omega L\chi'' + jL(\Delta\omega\omega_0 + \omega^2 4\pi\eta\chi')/\omega, \quad (3)$$

where  $\Delta\omega = 2(\omega - \omega_0)$ ,  $\Delta\omega \ll \omega_0$ , and  $(\omega^2 - \omega_0^2) \cong \Delta\omega\omega_0$ . The reflection coefficient  $\Gamma_R(\omega)$  near resonance of the cavity system with a paramagnetic sample will then be

$$\begin{aligned} \Gamma_R(\omega) &= [Z(\omega) - Z_0]/[Z(\omega) + Z_0] \\ &= \frac{R - Z_0 + \omega L 4\pi\eta\chi'' + j(\omega_0 L/\omega) [\Delta\omega + \omega 4\pi\eta\chi']}{R + Z_0 + \omega L 4\pi\eta\chi'' + j(\omega_0 L/\omega) [\Delta\omega + \omega 4\pi\eta\chi']} \end{aligned} \quad (4)$$

At the cavity resonance frequency  $\omega_0$ , the reflection coefficient  $\Gamma_{R0}$  becomes

$$\Gamma_{R0} = \frac{R - Z_0 + \omega_0 L 4\pi\eta(\chi'' + j\chi')}{R + Z_0 + \omega_0 L 4\pi\eta(\chi'' + j\chi')} \quad (5)$$

Using the definitions of  $Q_E$  and  $Q_U$ , Equation 5 may be written

$$\Gamma_{R0} = \frac{Q_E/Q_U - 1 + Q_E 4\pi\eta(\chi'' + j\chi')}{Q_E/Q_U + 1 + Q_E 4\pi\eta(\chi'' + j\chi')} \quad (6)$$

Equation 6 may be further simplified by using the reflection coefficient of the cavity at resonance without the paramagnetic sample,  $\Gamma_0$ ;  $\Gamma_0 = (R - Z_0)/(R + Z_0)$ , and the relation  $Q_E/Q_U = (1 + \Gamma_0)/(1 - \Gamma_0)$ : Thus

$$\Gamma_{R0} = \frac{2\Gamma_0 + Q_U(1 + \Gamma_0)(\chi'' + j\chi')4\pi\eta}{2 + Q_U(1 + \Gamma_0)(\chi'' + j\chi')4\pi\eta} \quad (7)$$

## SIGNAL DETECTION WITH LARGE CRYSTAL BIASING VOLTAGE

We will assume that we have a microwave bridge with a separate biasing and reference arm similar to the bridge shown in Figure 2. The voltage of the wave incident on the cavity is  $\hat{v}_1$ , which although generally a complex quantity, can be assumed to be real without loss of generality. The voltage reflected from the cavity is  $v_1 \Gamma_{R0}$ ; the voltage in the reference arm is  $\hat{v}_2 = v_2 e^{j\phi}$ . The voltages  $\hat{v}_1$ ,  $\hat{v}_2$ , and phase  $\phi$  can be adjusted by the appropriate attenuators and a phase shifter. The voltage  $\hat{v}_c$  at the crystal detector will be

$$\hat{v}_c = v_2 e^{j\phi} + v_1 \Gamma_{R0} \quad (8)$$

or substituting from Equation 7 for  $\Gamma_{R0}$ , we obtain

$$\hat{V}_c = V_2 e^{j\phi} + V_1 \left[ 2\Gamma_0 + Q_U (1 + \Gamma_0) (\chi'' + j\chi') 4\pi\eta \right] \times \left[ 2 + Q_U (1 + \Gamma_0) (\chi'' + j\chi') 4\pi\eta \right]^{-1} . \quad (9)$$

If we let

$$\xi = \frac{1}{2} Q_U (1 + \Gamma_0) 4\pi\eta \quad (10)$$

and assume that  $\xi\chi''$ ,  $\xi\chi' \ll 1$ , Equation 9 can be written

$$\hat{V}_c = V_2 e^{j\phi} + [V_1 \Gamma_0 + V_1 \xi (\chi'' + j\chi')] [1 - \xi (\chi'' + j\chi') + \xi^2 (\chi'' + j\chi')^2 + \dots] . \quad (11)$$

Retaining only terms of the second order of  $\chi''$  and  $\chi'$ , Equation 11 becomes

$$\hat{V}_c = V_2 e^{j\phi} + V_1 \Gamma_0 + (1 - \Gamma_0) V_1 \xi (\chi'' + j\chi') - (1 - \Gamma_0) V_1 \xi^2 (\chi'' + j\chi')^2 + \dots . \quad (12)$$

### Case 1: Large Bias, Absorption

The reference voltage is adjusted so that  $\phi = 0$  and  $V_2 > V_1 \Gamma_{R0}$ , and so that the detecting crystal is biased properly. Equation 12 then becomes (to the second order of  $\chi'$  and  $\chi''$ )

$$V_c = V_2 + V_1 \Gamma_0 + (1 - \Gamma_0) V_1 \xi (\chi'' + j\chi') - (1 - \Gamma_0) V_1 \xi^2 (\chi'' + j\chi')^2 . \quad (13)$$

The absolute voltage at the crystal,  $V_c$ , will be

$$V_c = (V_2 + V_1 \Gamma_0) + \zeta \chi'' + \zeta \xi (\chi'^2 - \chi''^2) + \left( \frac{1}{2} \right) \frac{\zeta^2 \chi'^2}{(V_2 + V_1 \Gamma_0)} , \quad (14)$$

where  $\zeta = (1 - \Gamma_0) V_1 \xi$ . In this case, the main signal is the absorption component of the RF susceptibility.

### Case 2: Large Bias, Dispersion

Bridge adjustment for observation of the dispersion signal is made by making  $\phi = 90$  degrees and  $\hat{V}_2 = V_2' e^{j\phi}$ . Note that  $V_2'$  of Case 2 and  $V_2$  of Case 1 are not necessarily equal, since the total bias voltage at the crystal must be the same in both cases. This condition depends on the reflected



power from the cavity. In this case Equation 12 becomes

$$\hat{V}_c = jV_2' + V_1 \Gamma_0 + \zeta(\chi'' + j\chi') - \zeta\zeta(\chi'' + j\chi')^2, \quad (15)$$

and the square of the absolute voltage at the crystal becomes

$$V_c^2 = V_2'^2 + V_1^2 \Gamma_0^2 + 2V_2' \zeta\chi' + 2\zeta V_1 \Gamma_0 \chi'' + \zeta^2 (\chi''^2 + \chi'^2) + 2\zeta\zeta V_1 \Gamma_0 (\chi'^2 - \chi''^2) - 4\zeta\zeta V_2' \chi'' \chi'. \quad (16)$$

With the same crystal bias for observation of absorption and dispersion signals, it follows from Equations 14 and 16 that we must have,

$$(V_2 + V_1 \Gamma_0)^2 = V_2'^2 + V_1^2 \Gamma_0^2, \quad (17)$$

or

$$V_2' = V_2 \left[ 1 + 2(V_1/V_2) \Gamma_0 \right]^{1/2}.$$

Substituting the value of  $V_2'$  into Equation 16, we obtain

$$\begin{aligned} V_c^2 = & (V_2 + V_1 \Gamma_0)^2 + 2V_2 \left[ 1 + 2(V_1/V_2) \Gamma_0 \right]^{1/2} \zeta\chi' + 2\zeta V_1 \Gamma_0 \chi'' + \zeta^2 (\chi''^2 + \chi'^2) \\ & + 2\Gamma_0 V_1 \zeta\zeta (\chi'^2 - \chi''^2) - 4V_2 \left[ 1 + 2(V_1/V_2) \Gamma_0 \right]^{1/2} \zeta\zeta \chi'' \chi'. \end{aligned} \quad (18)$$

The expression for  $V_c$  becomes quite cumbersome since the terms in  $\chi'$  and  $\chi''$  will generate further second-order terms. Retaining all second-order terms, we obtain

$$\begin{aligned} V_c = & V_b + \frac{\left[ 1 + 2(V_1/V_2) \Gamma_0 \right]^{1/2}}{V_b} V_2 \zeta\chi' + \frac{\Gamma_0}{V_b} V_1 \zeta\chi'' + \left( \frac{1}{2} \right) (1/V_b) \zeta^2 (\chi''^2 + \chi'^2) + \frac{\Gamma_0}{V_b} \zeta\zeta V_1 (\chi'^2 - \chi''^2) \\ & - \frac{1}{2} \frac{\left[ 1 + 2(V_1/V_2) \Gamma_0 \right]}{V_b^3} V_2^2 \zeta^2 \chi'^2 - \left( \frac{1}{2} \right) \frac{\Gamma_0^2}{V_b^3} V_1^2 \zeta^2 \chi''^2 - \left( \frac{1}{2} \right) \frac{\left[ 1 + 2(V_1/V_2) \Gamma_0 \right]^{1/2}}{V_b^3} \Gamma_0 V_1 V_2 \zeta^2 \chi'' \chi' \\ & - 2 \frac{\left[ 1 + 2(V_1/V_2) \Gamma_0 \right]^{1/2}}{V_b} V_2 \zeta\zeta \chi'' \chi', \end{aligned} \quad (19)$$

where  $V_b = (V_2 + V_1 \Gamma_0)$  is the bias voltage on the crystal. Equation 19 may be somewhat simplified if we assume that  $(V_1/V_2) < 1$ , and then disregard terms containing  $(V_1/V_2)$  of higher order than two.

Then Equation 19 becomes

$$\begin{aligned}
v_c = v_b + \frac{[1 + 2(v_1/v_2)\Gamma_0]^{1/2}}{v_b} v_2 \zeta_{X'} + \frac{\Gamma_0}{v_b} v_1 \zeta_{X''} + \left(\frac{1}{2}\right) (1/v_b) \zeta^2 (X''^2 + X'^2) \\
+ \frac{\Gamma_0}{v_b} v_1 \zeta \xi (X'^2 - X''^2) - \left(\frac{1}{2}\right) \frac{[1 + 2(v_1/v_2)\Gamma_0]}{v_b^3} v_2^2 \zeta^2 X'^2 - 2 \frac{[1 + 2(v_1/v_2)\Gamma_0]^{1/2}}{v_b} v_2 \zeta \xi_{X'} X'' \quad (20)
\end{aligned}$$

If  $(v_1/v_2)\Gamma_0 < (1/2)$ , we may write

$$v_c = v_b + \zeta_{X'} + \Gamma_0 \frac{v_1}{v_b} \zeta_{X''} + \left(\frac{1}{2}\right) (1/v_b) \zeta^2 (X''^2 + X'^2) + \Gamma_0 \frac{v_1}{v_2} \zeta \xi (X'^2 - X''^2) - \left(\frac{1}{2}\right) (1/v_b) \zeta^2 X'^2 - 2 \zeta \xi_{X'} X'' \quad (21)$$

## SIGNAL DETECTION WITH BALANCED BRIDGE

The next consideration is the so-called balanced-bridge case in which the microwave bridge is completely balanced except for a small unbalance in phase or amplitude to detect the dispersion or absorption signal. The resultant voltage at the detecting crystal is now small enough for operation of the crystal in the square-law region. Ordinarily, a magic "T" microwave bridge (Figure 1) lends itself readily to this type of operation, although there is obviously no reason why the bridge shown in Figure 2 cannot also be used for balanced bridge operation. The nomenclature developed for Cases 1 and 2 can therefore be easily transferred to the case of balanced bridge operation with no crystal bias. The voltage  $\hat{v}_2$  now simply becomes the voltage in the detecting arm of the crystal due to the power emanating from the reference arm of the bridge. Voltage  $\hat{v}_1$  is again the voltage due to the microwave power incident on the cavity.

### Case 3: Balanced Bridge, Absorption

To observe the  $X''$  signal, we let  $\phi = 180$  degrees in Equation 12 and make  $v_2 \cong v_1 \Gamma_0$  so that  $(v_2 - v_1)/v_2 \ll 1$  and the resonance signal  $\Delta V$  meets the condition  $\Delta V \ll (v_2 - v_1 \Gamma_0)$ . Then the expression for  $v_c$  will be the same for both Cases 1 and 3, except that the crystal bias  $(v_2 + v_1 \Gamma_0)$  of Equation 14 now becomes the bridge unbalance  $(v_1 \Gamma_0 - v_2)$ .

### Case 4: Balanced Bridge, Dispersion

Detection of  $X'$  for balanced-bridge operation is made with  $v_2 = v_1 \Gamma_0$ ,  $v_2 \ll \Delta V$ ,  $\phi = \Delta\phi + \pi$ ,  $\Delta\phi \ll 1$ . Referring again to Equation 12, we have

$$\hat{v}_c = -v_2 \left(1 + j\Delta\phi - \frac{1}{2} \Delta\phi^2\right) + v_1 \Gamma_0 + (1 - \Gamma_0) v_1 \xi (X'' + jX') - (1 - \Gamma_0) v_1 \xi^2 (X'' + jX')^2 \quad (22)$$

Using the balance condition  $(V_1 \Gamma_0 - V_2) = 0$ , we get for the magnitude of the voltage at the crystal

$$V_c = \Delta\phi V_2 - \zeta_X' + \left(\frac{1}{2}\right) \Delta\phi \zeta_X'' + \left(\frac{1}{2}\right) \zeta^2 \frac{X''^2}{\Delta\phi V_2} - \left(\frac{1}{8}\right) \frac{\Delta\phi \zeta^2}{V_2} X''^2 + \left(\frac{1}{2}\right) \zeta \Delta\phi (X'^2 - X''^2) + 2\zeta \zeta_X'' X' + \left(\frac{1}{2}\right) (1/V_2) \zeta^2 X'' X' , \quad (23)$$

where terms in first order of  $\Delta\phi$  are retained, and as before, of second order in  $X'$  and  $X''$ . Note here that the bridge unbalance to first order is  $j\Delta\phi V_2$ .

In Equations 14, 21, and 23, it can be seen that there is an admixture of dispersion and absorption for all cases, as already shown by Weger (Reference 1). However, Weger's analysis does not include second-order quantities shown in Equation 12 which are the result of the binomial expansion of Equation 7. Consequently, Cases 3 and 4, which correspond to Weger's Cases 2 and 3, respectively, differ in the number and magnitude of the higher-order terms containing  $X'$  and  $X''$ . For example, Case 3 can be compared with Weger's Case 2—the detection of  $X''$  by the balanced-bridge method. Weger concludes that a pure signal may be obtained by making the bridge unbalance large enough, (e.g.,  $X'^2/V_b \rightarrow 0$ ). Equation 14, however, clearly shows a term  $\zeta \Delta\phi (X'^2 - X''^2)$ , which cannot be eliminated by changing the bridge balance.

## OPTIMUM CAVITY REFLECTION COEFFICIENT AT RESONANCE AND CRYSTAL CHARACTERISTICS

So far we have considered the voltage  $V_c$  incident on the crystal, but not the crystal response. Let the response law be assumed to have the form

$$I \propto P_b^m \propto V_b^{2m} = V_b^n , \quad (24)$$

where  $P_b$  is the microwave bias power incident on the crystal,  $V_b$  the corresponding microwave voltage, and  $I$  the rectified crystal current. The crystal response to a small signal in the presence of a large signal,  $V_b$ , with  $I = f(V)$  expanded in a Taylor's series and with only the first term retained will be

$$\Delta S \propto n V_b^{n-1} \Delta V , \quad (25)$$

where  $\Delta S$  is the detected signal current and  $\Delta V$ , the change in microwave voltage due to resonance. The microwave bias voltage is derived either from the proper adjustment of the attenuator in the bias arm in Cases 1 and 2 or from the bridge unbalance in Cases 3 and 4. Table 1 summarizes the crystal biases and the resonance signals for the four cases. For Cases 1 and 2 the response  $\Delta S$  of

Table 1

## Crystal Biases and Resonance Signals.\*

Case	Crystal bias, $V_b$	Resonance signal, $\Delta V$
1	$(V_2 + V_1 \Gamma_0)$	$\zeta_X''$
2	$(V_2 + V_1 \Gamma_0)$	$\left[1 + 2(V_1/V_2)\Gamma_0\right]^{1/2} (V_2 + V_1 \Gamma_0)^{-1} \zeta_X' \approx \zeta_X'$
3	$(V_1 \Gamma_0 - V_2)$	$\zeta_X''$
4	$\Delta\phi V_2 = \Delta\phi V_1 \Gamma_0$	$-\zeta_X'$

\*See Equations 20, 21, and 23.

the crystal to  $\Delta V$  will be the same; i.e.,

$$\Delta S \propto n(V_2 + V_1 \Gamma_0)^{n-1} V_1 (1 - \Gamma_0^2) (Q_u/2) 4\pi\eta_X'' , \quad (26)$$

and similarly, for the detection of  $\chi'$ . Maximizing  $\Delta S$  with respect to  $\Gamma_0$ , we find

$$\Gamma_{0\max} = -\frac{(V_2/V_1)}{(n+1)} \pm \sqrt{\frac{(V_2/V_1)^2 + (n^2 - 1)}{(n+1)^2}} . \quad (27)$$

The optimum reflection coefficient for Case 3 is given by Equation 27 except that the first term is now positive. Case 4, interestingly enough, yields for the optimum  $\Gamma_0$ ,

$$\Gamma_{0\max} = \sqrt{(n-1)/(n+1)} . \quad (28)$$

Table 2 summarizes the values for the optimum reflection coefficient for the four cases considered above.

Goldsborough and Mandel have correctly pointed out the critical importance of the crystal response law on the optimum value of  $\Gamma_0$  (Reference 2). We have shown that this optimum value also depends on the ratio of the power in the sample and reference arms of the microwave bridge. The result is only partially appreciated in the calculations of Goldsborough and Mandel, because in their case (magic "T" microwave bridge) the power incident on the sample and that on the reference arm bear a constant ratio to each other. However, the "bias arm" microwave bridge configuration allows independent variation of power incident on the sample and the reference arm. In this case

Table 2

Values for Optimum Reflection Coefficient.

Case	Optimum reflection coefficient, $\Gamma_{0\max}$	
	$n = 2^*$	$n = 1^\dagger$
1 and 2	$-(1/3)(v_2/v_1) \pm (1/3) \left[ (v_2/v_1)^2 + 3 \right]^{1/2}$	$0, -(v_2/v_1)$
3	$+(1/3)(v_2/v_1) \pm (1/3) \left[ (v_2/v_1)^2 + 3 \right]^{1/2}$	—
4	$\sqrt{(1/3)}$	—

\*Although for Cases 1 and 2 detection is no longer "square law," the exponent  $n$  in Equation 24 is not necessarily 1; we have given the result for  $n = 2$ . Cases 3 and 4 are assumed to be strictly "square law."

<sup>†</sup>"Linear operation" applies to  $n = 1$ , and should apply to Cases 1 and 2 only.

the optimum reflection coefficient becomes a function of  $(v_2/v_1)$ .<sup>\*</sup> We also notice the interesting result that in Case 4—observation of  $\chi'$  with a balanced bridge—the optimum  $\Gamma_0$  is independent of  $(v_2/v_1)$ . This is the only case in which Feher's calculation (Reference 3) is strictly correct. Furthermore, Goldsbrough and Mandel's apparent tacit assumption—that the optimum reflection coefficient for Cases 3 and 4 is the same—is proved incorrect.

## CONCLUSIONS

The EPR signals obtained from a paramagnetic sample in a microwave bridge used either in the balanced bridge or "bias arm" configuration have been examined. Considerations of sensitivity aside, the observation of  $\chi'$  in the "bias arm" arrangement has the advantage that it can suppress all interference from first-order terms by simply increasing the bridge unbalance (Equations 21 and 23).<sup>†</sup> In the observation of  $\chi''$ , both types of bridge operation have interference signals that cannot be eliminated (Equation 14), for we find interference terms of order  $\chi''^2$  and  $\chi'^2$ . These second-order terms are both independent of and dependent on bridge balance. Here again, bridge-balance sensitive terms may be reduced by increasing the bridge bias (Case 1) or by increasing the bridge unbalance (Case 3). However, Equation 14 clearly shows that bridge bias operation allows the reduction of interference terms to negligible proportions.

Crystal detection and crystal operation in the linear and square-law range of the crystal detector has occasioned some confusion in EPR literature. Goldsbrough and Mandel have correctly

<sup>\*</sup> $(v_2/v_1)^2$  is directly proportional to the power ratio in sample and reference arm, respectively, if the waveguides are properly terminated and the cavity matched. However, this may not be the case; in fact for optimum signal,  $\Gamma_0 \neq 0$  for some cases.

<sup>†</sup>However, Weger<sup>(1)</sup> gives a method whereby  $\chi'$  can be detected in the balanced bridge operation without interference terms.

pointed out (Reference 2) that the paramagnetic signal is always detected linearly to the first order. However, the relatively large (i.e., relative to the signal) bias voltage on the crystal (derived either from a bridge unbalance or a separate bias arm arrangement) may be detected in the square-law region of the crystal characteristic. In addition, if the bias voltage is sufficiently large, it may also be detected in the so-called "linear region." It seems debatable whether crystal detection for large bias voltage is linear. A cursory check on a 1N23WE crystal (see Appendix A) operated in the linear range in a Varian electron spin resonance (ESR) spectrometer with a crystal bias current of approximately  $250\mu\text{a}$  shows the response of the crystal to be far from linear. Hence, operation of the bridge in the linear region will require an optimum cavity reflection coefficient which is not necessarily zero but will be more generally that given in Equation 27.

Goddard Space Flight Center  
National Aeronautics and Space Administration  
Greenbelt, Maryland, July 26, 1967  
120-33-01-11-51

## REFERENCES

1. Weger, M., *Bell System Tech. J.* 39:1013, 1960.
2. Goldsborough, J. P., Mandel M., *Rev. Sci. Instr.* 31:1044, 1960.
3. Feher, G., *Bell System Tech. J.* 36:449, 1957.
4. Buckmaster, H. A., Dering, J. C., *Can. J. Phys.* 43:1088, 1965.
5. Beringer, R., "The Measurement of Wavelength," in: *Technique of Microwave Measurements*, Mass. Inst. of Tech., Radiation Lab. Series, Vol. 11, ed. by C. G. Montgomery, New York: McGraw-Hill Book Co. Inc., 1947.
6. Beringer, R., "Resonant Cavities as Microwave Circuit Elements," in: *Principles of Microwave Circuits*, Mass. Inst. of Tech., Radiation Lab. Series, Vol. 8, ed. by C. G. Montgomery, R. H. Dicke, E. M. Purcell, New York: McGraw-Hill Book Co. Inc., 1948.
7. Bloembergen, N., "Nuclear Magnetic Relaxation," New York: W. A. Benjamin, 1961.
8. Robbins, R. C., and Black, F. W., "An Investigation into the Use of Crystal Rectifiers for Measuring and Monitoring Purposes," *Journal of the Institution of Electrical Engineers* 93 (Part IIIA): 1343, March-May 1946.

## Appendix A

### 1N23WE Crystal Characteristics

The crystal characteristic of a 1N23WE diode was checked in the 3.4- to 2000-microwatt range. This large power range could not be covered with a single detecting instrument. Figure A1 shows the detecting circuits used. It is usually stated in the literature that rectified crystal current is proportional to the RF power for power levels less than  $10^{-5}$  watt, and proportional to the square root of the RF power for power levels greater than  $10^{-4}$  watt (Reference 3). Very little experimental data are given in support of these figures. The usual source is Robbins and Black (Reference 8), who investigated silicon rectifiers designed for centimeter wavelength at 50 Hz and 200 MHz.

It is difficult to see how data obtained at 200 MHz can be extrapolated with any confidence to 10,000 MHz. Curve A in Figure A1 was taken in a power range used in Varian Associates electron spin resonance spectrometers at a frequency of 9.7 GHz. The audio detecting circuit is almost identical to the Varian Associates audio input circuit. The recommended bias current of 250 microamperes supposedly results in linear operation of the crystal (1N23F in the Varian V-4500-41A X-band microwave bridge). Curve A shows that operation in the 100- to 300-microampere region is approximately square-law (actually  $I \propto V^{2.5}$ ). In fact, linear operation is not closely approached in the range from  $10^{-3}$  to  $10^{-4}$  watt; therefore, the author's misgivings about calculations of the optimum cavity reflection coefficient in the "linear region" are justified. However, the experimental curves in Figure A1 should be used with caution, since crystal characteristics are a function of the dc load impedance (Reference 8). This is also evident if one compares Curves A and B in the 160-microwatt region.

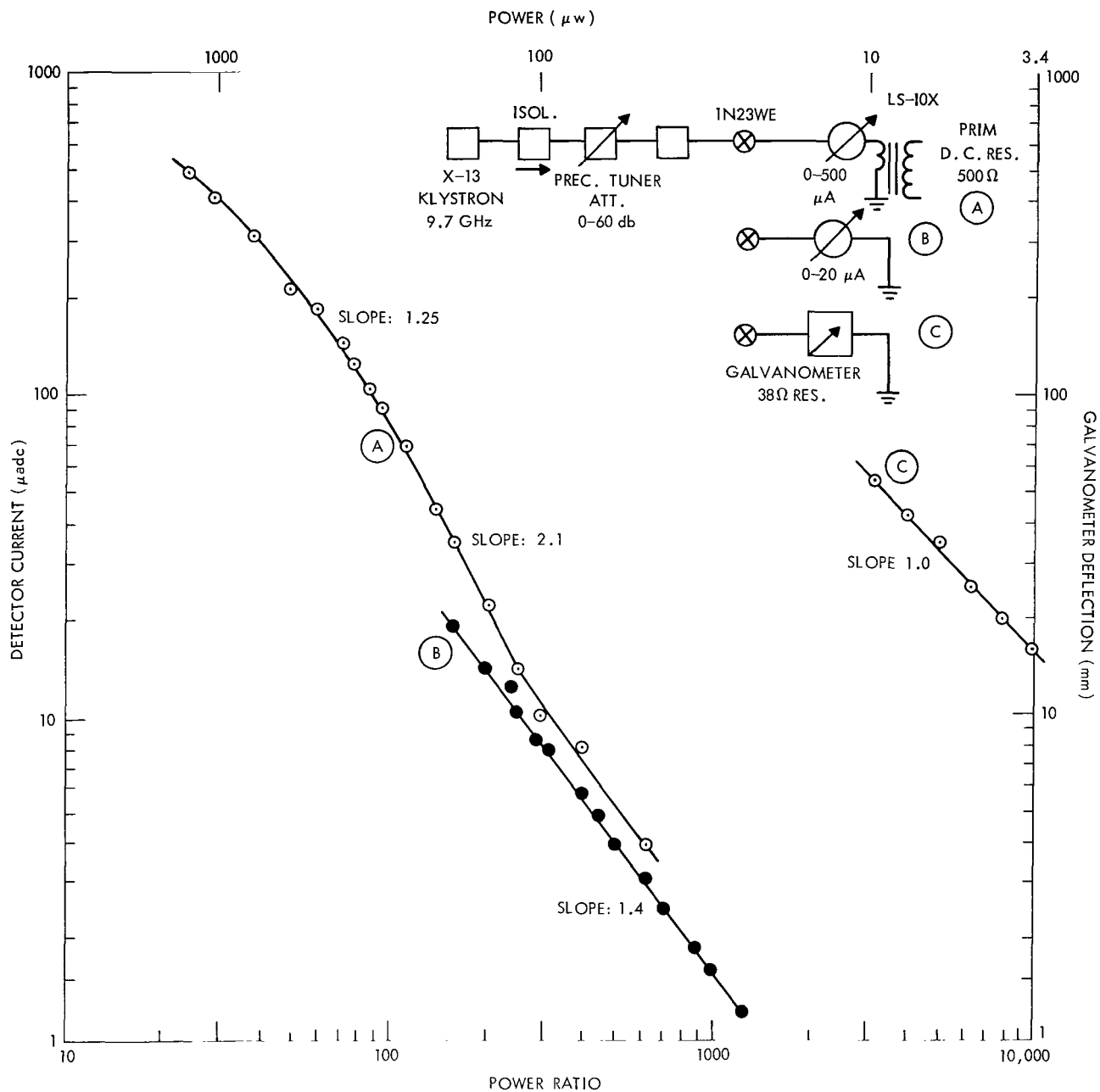


Figure A1—1N23WE detector current vs. X-band (9.7 kHz) microwave power.



000 001 30 01 30S 00092 00 003  
NATIONAL AERONAUTICS AND SPACE ADMINISTRATION  
WASHINGTON, D. C. 20546

LIBRARY 7/11/67

POSTMASTER: If Undeliverable (Section 158  
Postal Manual) Do Not Return

*"The aeronautical and space activities of the United States shall be conducted so as to contribute . . . to the expansion of human knowledge of phenomena in the atmosphere and space. The Administration shall provide for the widest practicable and appropriate dissemination of information concerning its activities and the results thereof."*

—NATIONAL AERONAUTICS AND SPACE ACT OF 1958

## NASA SCIENTIFIC AND TECHNICAL PUBLICATIONS

**TECHNICAL REPORTS:** Scientific and technical information considered important, complete, and a lasting contribution to existing knowledge.

**TECHNICAL NOTES:** Information less broad in scope but nevertheless of importance as a contribution to existing knowledge.

**TECHNICAL MEMORANDUMS:** Information receiving limited distribution because of preliminary data, security classification, or other reasons.

**CONTRACTOR REPORTS:** Scientific and technical information generated under a NASA contract or grant and considered an important contribution to existing knowledge.

**TECHNICAL TRANSLATIONS:** Information published in a foreign language considered to merit NASA distribution in English.

**SPECIAL PUBLICATIONS:** Information derived from or of value to NASA activities. Publications include conference proceedings, monographs, data compilations, handbooks, sourcebooks, and special bibliographies.

**TECHNOLOGY UTILIZATION PUBLICATIONS:** Information on technology used by NASA that may be of particular interest in commercial and other non-aerospace applications. Publications include Tech Briefs, Technology Utilization Reports and Notes, and Technology Surveys.

*Details on the availability of these publications may be obtained from:*

SCIENTIFIC AND TECHNICAL INFORMATION DIVISION  
NATIONAL AERONAUTICS AND SPACE ADMINISTRATION

Washington, D.C. 20546